molecular pharmaceutics

Article

Cite This: *Mol. Pharmaceutics* 2019, 16, 4230−4240

pubs.acs.org/molecularpharmaceutics

Comprehensive Evaluation of Bile Acid Homeostasis in Human Hepatocyte Co-Culture in the Presence of Troglitazone, Pioglitazone, and Acetylsalicylic Acid

Jae H. Chang,*,† Dewakar Sangaraju,† Ning Liu, Allan Jaochico, and Emile Plise

Genentech, Inc, South San Francisco, California 94080, United States

Supporting Information

ABSTRACT: Interruption of bile acid (BA) homeostasis has been hypothesized for a variety of liver diseases and for drug-induced liver injury (DILI). Consequently, BA is gaining increasing prominence as a potential biomarker. The objective of this work was to evaluate the effect of troglitazone (TZN, associated with severe DILI), pioglitazone (PZN, rarely associated with DILI), and acetylsalicylic acid (ASA, or aspirin, not associated with DILI) on the in vitro BA homeostasis in hepatocytes co-cultured with nonparenchymal cells by monitoring the disposition of 36 BAs. The cells were supplemented with 2.5 μM d_4-cholic acid, d_4-chenodeoxycholic acid, d_4-lithocholic acid, d_4-deoxycholic acid, d_4-ursodeoxycholic acid, and hyodeoxycholic acid. Concentration−time profiles of BAs were used to determine the area under the curve from the supernatant, lysate, or bile compartments, in the presence or absence of TZN, PZN, or ASA. When applicable, IC_{50} describing depletion of individual BAs was calculated, or accumulation greater than 200% of dimethyl sulfoxide control was noted. Thiazolidinediones significantly altered the concentration of glycine and sulfate conjugates; however, more BAs were impacted by TZN than with PZN. For commonly shared BAs, TZN exhibited 3- to 13-fold stronger inhibition than PZN. In contrast, no changes were observed with ASA. Modulation of BA disposition by thiazolidinediones and ASA was appropriately differentiated. Particularly for thiazolidinediones, TZN was more potent in interrupting BA homeostasis, and, when also considering its higher dose, may explain differences in their clinical instances of DILI. This is one of the first works which comprehensively evaluated the disposition of primary and secondary BAs along with their metabolites in an in vitro system. Differing degrees of BA homeostasis modulation was observed with various perpetrators associated with varying clinical instances of DILI. These data indicate that in vitro systems such as hepatocyte co-cultures may be a promising tool to gain a detailed insight into how drugs affect BA handling to further probe into the mechanism of DILI related to BA homeostasis.

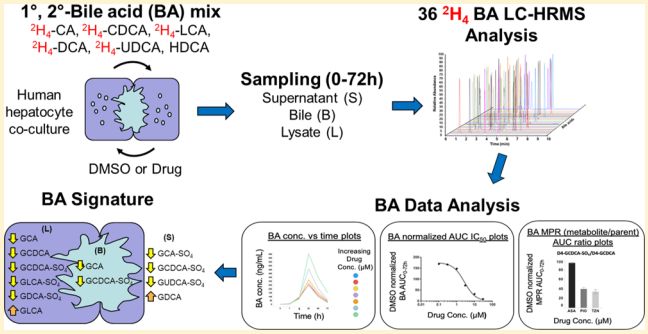

KEYWORDS: *acetylsalicylic acid, bile acids, drug-induced liver injury, hepatocytes, hepatotoxicity, pioglitazone, troglitazone*

INTRODUCTION

Drug-induced liver injury (DILI) is one of the major safety liabilities encountered during drug development. In fact, hepatotoxicity is one of the primary causes for drugs being withdrawn from the market,[1] and has been responsible for many post-marketing warnings and restrictions.[2] For example, whereas in silico approaches offer promise, its application is currently hampered by incomplete understanding of the mechanisms of DILI, complexity because of multiple factors contributing to DILI, and the limited availability of high-quality clinical data.[3,4] Similarly, for in vitro assessment of hepatotoxicity, even when a multifactorial process was taken to integrate several in vitro datasets, DILI risk could not be clearly differentiated between drugs.[5,6] Consequently, application of modeling and simulations tools which incorporate in silico and in vitro data have been used to primarily study the mechanism of DILI for a particular drug,[7] rather than being widely utilized as a prospective tool to assess DILI. In vivo, animal models were not much better as they failed to capture more than 40% of hepatotoxicity observed in humans.[8] To exacerbate the matter, studies indicated that controlled clinical studies may not be adequate to derisk hepatotoxicity. For example, false positives, as measured by increases in liver transaminase levels, were reported with the placebo group in phase 1;[9] whereas, hepatotoxicity with fialuridine was not discovered until phase 2.[10] As the pursuit of a more suitable tool and methodology to evaluate DILI continues, investigation into clinical biomarkers more specific and sensitive for DILI has emerged. In particular, bile acids (BAs) may be a potential biomarker that can be utilized during drug development to prospectively identify DILI risk.

Received: May 23, 2019
Revised: August 12, 2019
Accepted: September 11, 2019
Published: September 11, 2019

DOI: 10.1021/acs.molpharmaceut.9b00562
Mol. Pharmaceutics 2019, 16, 4230−4240

BAs are amphipathic molecules which are products of cholesterol metabolism mediated by multiple enzymes including cytochrome (CYP) P450 such as CYP7A1, CYP27A1, and CYP8B1. The primary BAs cholic acid (CA) and chenodeoxycholic acid (CDCA) are generated in the liver. Whereas these primary BAs can be directly amidated or conjugated, they are mostly shunted into the intestine via the bile canaliculi, which leads to the formation of secondary BAs such as deoxycholic acid (DCA), lithocholic acid (LCA), urosodeoxycholic acid (UDCA), and hyodeoxycholic acid (HDCA). BAs are shuttled between the liver and the intestine, and will eventually undergo further metabolism through conjugation biotransformation reactions mostly involving glycine, taurine, or sulfate. In humans, the ratio of glycine- to taurine-conjugate was 3.2,[11] and this ratio varies across preclinical species as it is highly species-dependent.[12] In general, LCA is considered the most hydrophobic species followed by BAs containing di-hydroxyl moieties such as CDCA, DCA, UDCA, and HDCA. BAs containing tri-hydroxyl moieties such as CA are the most hydrophilic species.

There are several reasons why BAs may be a suitable biomarker for DILI. One reason is because the liver is a key organ in maintaining BA homeostasis; any changes in liver physiology should impact BA levels. In fact, interruption of BA homeostasis has been reported for liver diseases including hepatitis, jaundice, and cirrhosis,[13−16] as well as for DILI.[17,18] In addition, concentrations of BAs are typically high and, more importantly, can be found in circulation and in biological matrices including urine. Therefore, noninvasive methods can be used to easily monitor BAs. The utility of BAs as a biomarker was initially challenging because of technical limitations in quantitating the structurally diverse array of BAs and their metabolites. However, with the advent of high-performing mass spectrometers, quantitation of individual BA species has become more feasible.[19,20] The objective of this work was to evaluate the effect on the in vitro BA homeostasis by drugs associated with differing instances of clinical DILI in a compartmentalized in vitro system exhibiting metabolic and drug transporter function. Comprehensive analysis was conducted by monitoring the disposition of 36 BAs using liquid chromatography−high-resolution mass spectrometry (LC−HRMS). Hurel, a human hepatocyte co-culture, was employed because it overcame certain challenges encountered with other systems such as reduced metabolic and drug transporter function,[21−23] as well as enabling access to the bile and intracellular compartments to study the disposition of BA.[24] In addition, Hurel afforded seeding hepatocytes at higher cellular density, which ensured that adequate amounts of BAs were collected to aid in their quantitation on the LC−HRMS. Finally, the ability to establish a long-enduring culture without the addition of artificial supplements such as Matrigel, which may affect the free concentration of BAs and/or the perpetrators as well as potentially impeding adequate transfer of nutrients and oxygen to hepatocytes,[25] or without the need to regularly change the media to enable continuous monitoring of BA disposition,[26] further distinguished it from other in vitro systems. The impact of troglitazone (TZN, thiazolidinedione class drug, which was withdrawn from the market because of severe DILI), pioglitazone (PZN, thiazolidinedione class drug, which is rarely associated with DILI), and acetylsalicylic acid (ASA, or aspirin, a drug which is not commonly associated with DILI), on the effect of individual BAs and their metabolites was investigated.

MATERIALS AND METHODS

Materials. TZN was purchased from Toronto Research Chemicals (North York, ON, Canada). PZN was purchased from Aldrich Chemistry (Milwaukee, WI). Rotenone was purchased from EMD Millipore (Burlington, MA). ASA and sterile dimethyl sulfoxide (DMSO) were purchased from Sigma-Aldrich (St. Louis, MO). $^2H_4$-cholic acid (d_4-CA), $^2H_4$-chenodeoxycholic acid (d_4-CDCA), $^2H_4$-lithocholic acid (d_4-LCA), and $^2H_4$-deoxycholic acid (d_4-DCA) were purchased from Steraloids, Inc. (Newport, RI). All authentic unlabeled BA standards (parent, glycine conjugates, taurine conjugates, and sulfate conjugates) were purchased from commercial sources such as Steraloids, Inc. (Newport, RI) or Sigma-Aldrich (St. Louis, MO, USA). $^2H_4$-ursodeoxycholic acid (d_4-UDCA) was purchased from Cerilliant Corporation (Round Rock, TX). HDCA was purchased from Steraloids, Inc. (Newport, RI). CellTiter-Glo cell viability (G7571) and LDH-Glo (J2380) cytotoxicity assays were purchased from Promega Corporation (Madison, WI).

Hμrelflux 24-well kits (hepatocyte lots HU1013, HU1020, and HU1023) are human hepatocytes co-cultured with nonparenchymal cells that were purchased from Hμrel Corporation (North Brunswick, NJ). HU1013 was from a Caucasian male aged 65 whose cause of death was stroke. HU1020 was from a Caucasian male aged 49 whose cause of death was exsanguination. HU1023 was from a Caucasian male aged 48 whose cause of death was cerebrovascular/stroke.

Disposition of BAs and Their Metabolites in Hepatocyte Co-Culture. The hepatocyte co-culture experiment was conducted as described in the protocol provided by Hμrel Corporation. Briefly, Hμrelflux 24-well kits containing single-donor lots of human hepatocytes (1.88×10^5 cells/well) were co-cultured with nonparenchymal stromal cells at Hμrel Corporation and shipped to Genentech. It is assumed that these support cells are metabolically incompetent and do not play a role in active transport. Approximately on the 7th day following initial seeding, the cells were received and equilibrated in reagent A (hepatocyte dosing medium) for 1−2 h at 37 °C, 5% CO_2, and 90% humidity. Co-cultures were dosed with 0.4 mL of sterile filtered (0.22 μm) reagent A containing 2.5 μM each of d_4-CA, d_4-CDCA, d_4-LCA, d_4-DCA, d_4-UDCA, and HDCA, as well as DMSO control and the perpetrating drugs TZN (0.1−30 μM), PZN (0.1−100 μM), or ASA (3−1000 μM). It is assumed that the metabolism and flux of the BAs are not altered with the deuterium label. Because the data analysis is comparing drug-treated cells with DMSO control, the impact would be minimal in the data analysis even if the deuterium label affected the disposition of the BAs. Total DMSO concentration did not exceed 0.6%. At 0, 1, 3, 24, 48, and 72 h following addition of reagent A incubation mix, the medium was collected and the cells were washed once at 4 °C with 0.8 mL reagent A (wash buffer). The biliary canaliculi were also opened by incubating the cells at 37 °C for 20 min in 0.4 mL reagent B (Hurel tight junction disruption reagent). Cells were lysed in 0.4 mL methanol/water (70:30 v/v) and scraped to ensure lysis. All samples were stored at −80 °C prior to LC−HRMS analysis. Intracellular concentrations were normalized to the total number of hepatocytes in each well, which was 1.88×10^5 cells. Each bile compartment was assumed to be a sphere with a radius of 1 μm.[27] Bile concentrations were normalized to the total apparent bile volume, accounting for the 400 μL dilution with

DOI: 10.1021/acs.molpharmaceut.9b00562
Mol. Pharmaceutics 2019, 16, 4230−4240

buffer used during the bile extraction phase. TZN experiments with lot HU1013 were run in three independent experiments to assess interday reproducibility. TZN experiments with lots HU1023 and HU1020 were run as single independent experiments. Experiments with PZN and ASA with lots HU1013 and HU1020 were run as two independent experiments.

Viability and Cytotoxicity Assays. Hμrelflux hepatocytes from lot HU1013 were dosed (n = 3) with DMSO, TZN (10 and 100 μM), PZN (30 and 100 μM), ASA (100 and 1000 μM), and rotenone (positive control, 20 μM) and incubated at 37 °C for approximately 72 h. LDH levels were determined in reagent A according to the manufacturer's protocol. Briefly, medium was diluted 100-fold in LDH storage buffer (200 mM Tris-HCl, 10% glycerol, 1% bovine serum albumin, pH 7.3). After a 45 min incubation at room temperature, luminescence readings were recorded on a SpectraMax i3 (Molecular Devices, Sunnyvale, CA) using an integration time of 750 ms per well as recommended in the protocol. ATP levels were determined according to the manufacturer's protocol with minor modification to accommodate increased volumes of the 24-well plates. The 24-well plate was allowed to reach room temperature before CellTiter-Glo reagent (0.4 mL) was added to 0.4 mL of cell culture medium reagent A. The plate was shaken at 120 rpm for 2 min to induce cell lysis before being incubated at room temperature for 10 min to allow luminescence to stabilize. Luminescence readings were recorded on a SpectraMax i3 using an integration time of 300 ms per well as recommended in the protocol.

Sample Analysis. The sample (100 μL) from the supernatant, bile, or lysate compartment was precipitated with 400 μL of acetonitrile followed by centrifugation at 3000 rpm for 10 min at 4 °C. The sample (450 μL) was then dried under nitrogen and reconstituted with 100 μL of mobile phase A for LC tandem HRMS analysis. Pooled QC samples were prepared by combining 10 μL from the corresponding supernatant, bile, or lysate samples, and 100 μL volume was processed in the same manner as the above samples. Batch analysis included authentic standard curves in a surrogate matrix (methanol) using a pool of unlabeled parent and metabolized BA analytes, separate pool QCs (N = 3) interspersed at the beginning, middle, and end of the supernatant, bile, and lysate samples. Pool QCs were prepared by pooling an equal volume of sample from each sample (supernatant, bile, and lysate separately) and analyzed in every batch for sample analysis. All samples from DMSO and varying drug concentration treatment were analyzed together as a single batch. Authentic standard curve samples were prepared using a pool of all BA analytes in methanol at 1.0, 10.0, 100.0, 1000.0, 2500.0, 5000.0 ng/mL, and 100 μL processed in the same manner as the above samples. Standard curves were plotted using peak areas of the analytes versus actual concentration with $1/X^2$ weighting. Standard curves were used to calculate deuterated BA species at various time points. % relative standard deviation (% RSD = standard deviation/average × 100) was determined to assess overall batch performance. Although, surrogate matrix (methanol) curves were used for quantitation, all IC_{50} and metabolite-to-parent ratio (MPR) calculations were normalized to corresponding DMSO control samples, eliminating any matrix effects that may arise during LC−HRMS analysis.

LC−HRMS analysis was performed on a Shimadzu series ultra-high-performance LC (UHPLC) system (Shimadzu, Kyoto, Japan) connected to an Orbitrap—Q Exactive HF-X instrument (Thermo Fisher Scientific, Waltham, MA USA). The UPLC system consisted of LC pumps (model LC-30AD) with an online degasser to deliver the LC mobile phases A: 10 mM ammonium acetate and 0.1% v/v ammonium hydroxide in 50:50 v/v water/methanol, and mobile phase B: 10 mM ammonium acetate and 0.1% v/v ammonium hydroxide in methanol at a flow rate of 0.35 mL/min. The samples (7.5 μL) were injected using an autosampler (model SIL30ACMP) maintained at 15 °C. A Waters Acquity BEH C18, 100 × 2.1 mm, 1.7 μm particle size, UPLC reverse phase column (Waters Corp., Milford, MA) was used for LC separation. Gradient LC flow started with 5% B for 0.5 min, followed by a linear increase to 20% B in 3 min; to 50% B in 2 min; to 65% B in 2 min; to 85% B in 0.5 min. The 85% B was held for another 0.5 min before returning to 5% B, which was held for 1 min to re-equilibrate the LC column. Total run time was 10 min and column oven (model CTO30A) temperature was maintained at 50 °C.

HRMS analysis was performed on Orbitrap—Q Exactive HF-X instrument or Q Exactiveplus (Thermo Fisher Scientific, Waltham, MA USA) in full scan mode using electrospray ionization (ESI) in negative ion mode. MS scan range was set to mass to charge ratio (m/z) of 100 to 1000 at a resolution of 120 000 or 70 000 (full width at half-maximum), automatic gain control target value of 1×10^6, maximum injection time of 200 ms with profile mode data acquisition. MS source parameters included a heated ESI probe with spray voltage of 2.5 kV, sheath gas flow rate of 49 mL/min, auxiliary gas flow rate of 12 mL/min, sweep gas flow rate of 2 mL/min, capillary temperature of 259 °C, and funnel radio frequency (RF) level at 80.0. Data processing was performed using TraceFinder 4.1 software (Thermo Fisher Scientific, Waltham, MA USA), which involved peak picking, integration, and plotting standard curves using the BA compound database. $(M - H)^-$ m/z ratio peaks of all stipulated BA species were consistently extracted and integrated from full scan data within 5 ppm mass accuracy. Unknown concentrations of individual d_4-BAs in the samples were calculated from the standard curve slope of corresponding individual BAs. Levels below 1 ng/mL or MS peak area below 1×10^5 was considered below the limit of quantitation.

Data Analysis. Concentration−time profile was determined for each d_4-BA and its metabolites. Because the concentration−time profile was dependent on a particular BA species, area under the curve (AUC) was calculated using standard trapezoid rule calculated with Excel using all measurable timepoints from the first (0 h) and last timepoint (72 h). Changes in AUC were compared between DMSO control and perpetrating drugs TZN, PZN, and ASA. When possible, IC_{50} was determined to describe the depletion of BAs using PRISM 7 (GraphPad, San Diego, CA)

$$Y = \text{bottom} + (\text{top} - \text{bottom}) / (1 + 10^{((\log IC_{50} - X) \times \text{hillslope})})$$

where X is the nominal concentration of the perpetrators evaluated in the hepatocyte co-culture and Y is % AUC change. Nonlinear regression involved variable slope with four parameters fitting and bottom constraint as 0. The quality of the fit was assessed by $R^2 > 0.7$ and that the BA concentrations were above the limit of detection (i.e., AUC > 0.1 ng/mL·h), while ensuring that the extent of inhibition was >50% of DMSO control.

DOI: 10.1021/acs.molpharmaceut.9b00562
Mol. Pharmaceutics 2019, 16, 4230−4240

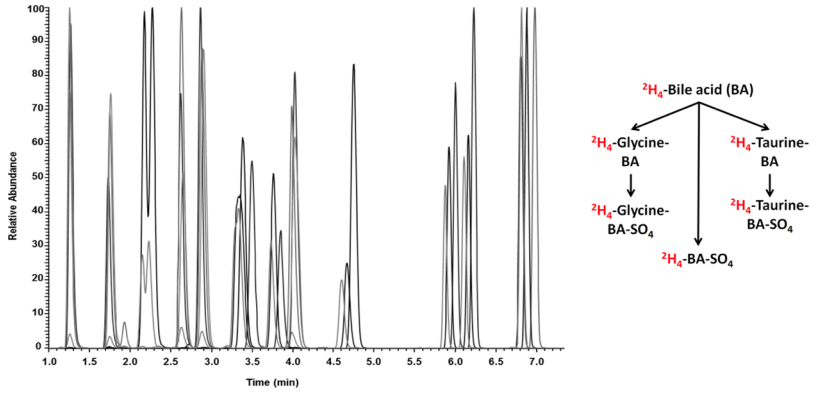

Figure 1. Representative chromatogram of BAs and their metabolites using LC−HRMS. The inset illustrates all the potential metabolites that are associated with a particular BA.

RESULTS

Characterizing Endogenous Distribution of BAs and Their Metabolites in Vitro. LC−HRMS profiling was used to determine the concentrations of all BAs and their metabolites (Figure 1). Analysis included standard curves which were used to determine unknown concentrations of BAs and their metabolites at various time points in all samples. Sample pool QCs injected across the batch in all compartments (N = 3 each) were used to assess sample batch performance and their MS peak area. % RSD was less than 25% in all batches, indicating overall good batch performance.

The concentration of endogenous BAs and their metabolites was determined. In this system, only low levels of GCA, GCDCA, TCA, and TCDCA were observed. Secondary BAs were not observed, which is consistent with the fact that secondary BAs are byproducts of intestinal metabolism. Because the desire was to replicate physiological conditions, a cocktail containing deuterated primary BAs (d_4-CA and d_4-CDCA) and secondary BAs (d_4-LCA, d_4-DCA and d_4-UDCA) was supplemented. The reason why deuterated BAs were utilized was to discern between endogenous and exogenous BAs and their metabolites. In addition to the deuterated BAs, nondeuterated HDCA was included in the cocktail because d_4-HDCA was not commercially available and because it was assumed that nonlabeled HDCA would not interfere with analysis as HDCA-related analytes were not found endogenously.

Several concentrations of the cocktail were evaluated to optimize the in vitro condition. The concentration of the cocktail was targeted to ensure robust quantitation on the LC−HRMS, and to mirror the proportion of BA and their metabolites found in human serum, but not too high as to perturb the system with a sudden influx of exogenous BAs. Figure 2A shows that the cocktail containing 2.5 μM of individual primary and secondary BAs (where the total exogenous BA concentration is 15 μM) yielded BA proportions in the supernatant that was comparable to what was reported in human serum. The proportion of all species related to d_4-CA in the supernatant was the highest at around 35%, followed by d_4-UDCA at 23%, d_4-DCA at 16%, d_4-CDCA at 16%, d_4-HDCA at 9%, and d_4-LCA at 2%. Assuming that the supernatant reflects the plasma compartment in vivo, these proportions are within reasonable proximity with what is reported in the literature in human serum.[20] For the BA conjugates, Figure 2B shows that the proportion of all glycine conjugates was highest at around 62%, followed by sulfate conjugates at 37% and taurine conjugates at 1%, and ranked ordered appropriately to what is reported in human serum.[20]

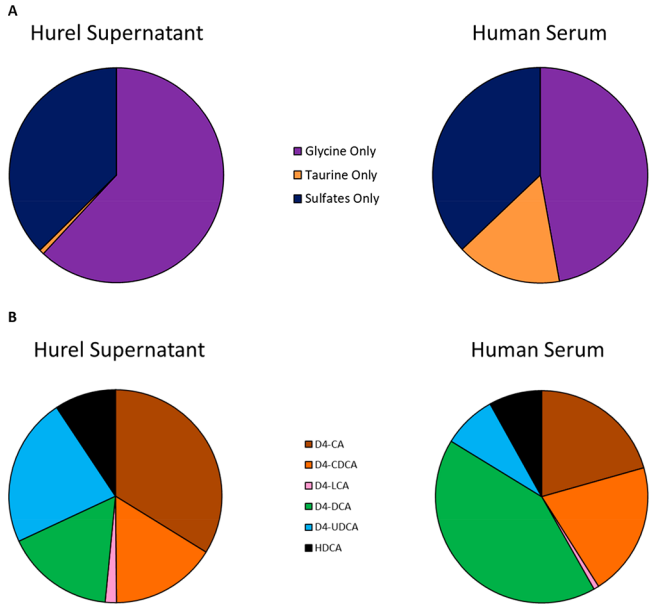

Figure 2. Pie charts summarizing the relative proportion of (A) unconjugated primary and secondary BAs and (B) glycine, taurine, and total sulfated metabolites, which includes sulfation of amidated BAs in the supernatant of lot HU1013 compared with reported literature data in human serum.[20] The relative proportions were calculated from AUC determined from 0 to 72 h.

Concentration−Time Profile of BAs and Their Metabolites in Vitro. Following the addition of the cocktail, BAs and their metabolites were monitored in lot HU1013 for over 72 h. Representative concentration−time profiles for CDCA and its metabolite are shown in Figure 3, and data for other BAs and their metabolites are shown in Figure S1. In general, the primary and the secondary BAs were quickly taken up by the cells and distributed into the bile. BAs were completely depleted by 24−48 h in all compartments. When considering the relative hydrophobicity of BAs, d_4-LCA is the most hydrophobic BA and, as expected, is rapidly metabolized within 3 h, whereas the rate of metabolism for the more hydrophilic BA such as CA is not completely metabolized until 24 h, underscoring the relevance of this system to study BA homeostasis. In the meantime, amidation of primary BAs peaked between 24 and 48 h in all compartments, except for

DOI: 10.1021/acs.molpharmaceut.9b00562
Mol. Pharmaceutics 2019, 16, 4230−4240

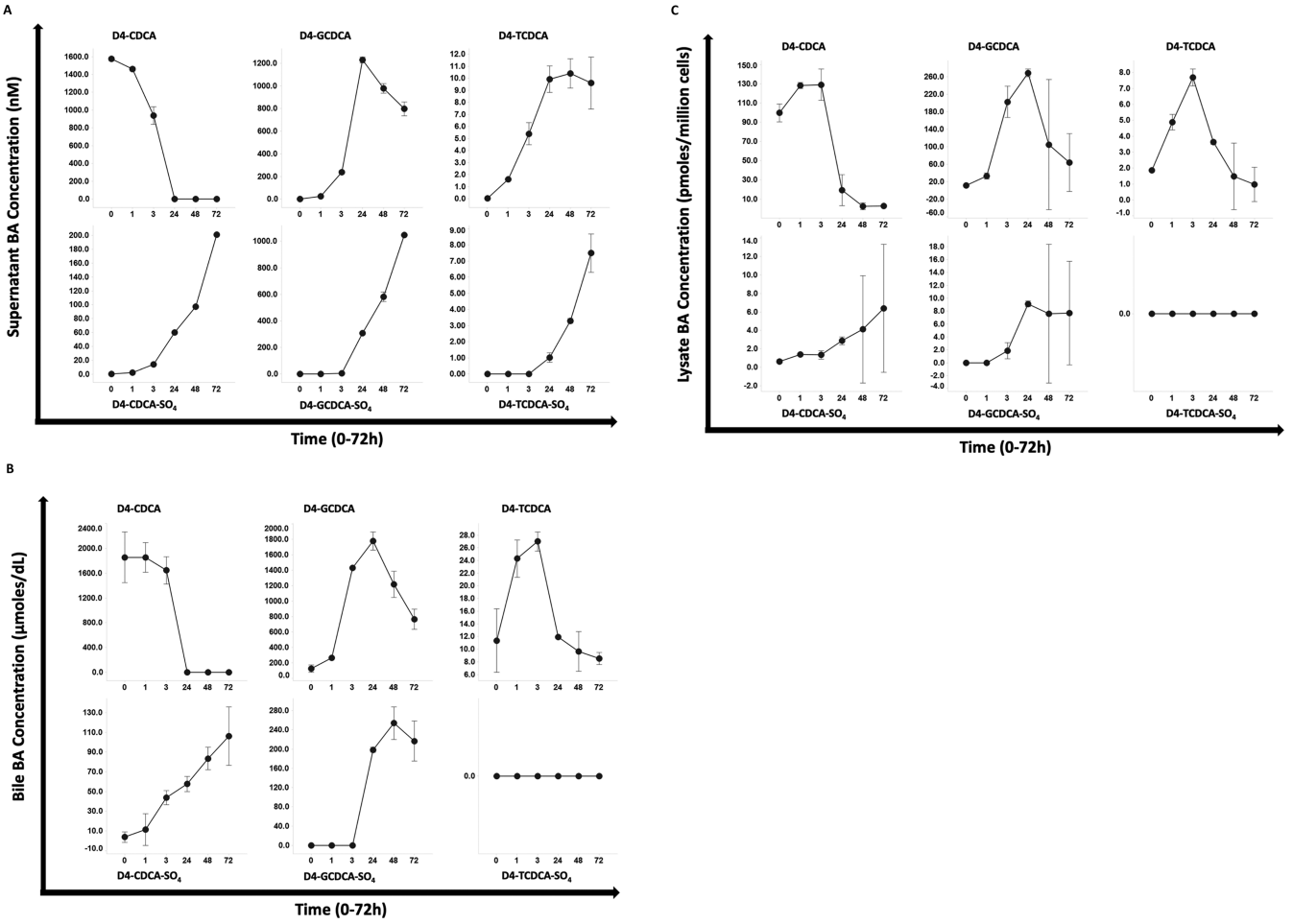

Figure 3. Representative concentration−time profile of CDCA and its conjugated metabolites in the (A) supernatant, (B) lysate, and (C) bile in lot HU1013 over 72 h. Concentration−time profile for other BAs and their metabolites are in Figure S1.

Table 1. Summary of Changes in the Concentration of BAs and Their Metabolites Reported as IC_{50} (μM) in the Absence or Presence of Ascending Concentrations of TZN (0.1−30 μM), PZN (0.1−100 μM), or ASA (3−1000 μM)[a]

Bile acids		Primary & Secondary						Glycine conjugates						Taurine conjugates						Sulfate conjugates															
		D4-CA	D4-CDCA	D4-LCA	D4-DCA	D4-UDCA	HDCA	D4-GCA	D4-GCDCA	D4-GLCA	D4-GDCA	D4-GUDCA	GHDCA	D4-TCA	D4-TCDCA	D4-TLCA	D4-TDCA	D4-TUDCA	THDCA	D4-CA-SO4	D4-CDCA-SO4	D4-LCA-SO4	D4-DCA-SO4	D4-UDCA-SO4	HDCA-SO4	D4-GCA-SO4	D4-GCDCA-SO4	D4-GLCA-SO4	D4-GDCA-SO4	D4-GUDCA-SO4	GHDCA-SO4	D4-TCA-SO4	D4-TCDCA-SO4	D4-TLCA-SO4	D4-TDCA-SO4	D4-TUDCA-SO4	THDCA-SO4
Troglitazone	Supernatant										*															10 ± 6	21 ± 12			26 ± 8						
	Bile							16 ± 1																			27 ± 10										
	Lysate							5.6 ± 2.9	11 ± 12	*																	5.1 ± 2.1	2.6 ± 0.7	3.9 ± 1.3									
Pioglitazone	Supernatant										*															27 ± 1	95 ± 49										
	Bile																																				
	Lysate					74 ± 28		33 ± 32	40 ± 12	*		19 ± 0.2																35 ± 10	37 ± 26								
Aspirin	Supernatant, Bile, Lysate	No signifinant Bile acids inhibition or accumulation observed																																	
		No significant Bile acids inhibition or accumulation observed																																	
		No significant Bile acids inhibition or accumulation observed																																	

IC50 < 20 µM; IC50 20-100 µM; * Bile acid accumulation observed; No Bile acids inhibition observed

[a]IC_{50}s were calculated based on change in AUC between DMSO control and TZN. Star (*) represents BAs or their metabolites which exhibited >200% accumulation over 72 h. All experiments were conducted in lot HU1013. Results for TZN are reported as mean ± SD of three independent measurements with criteria outlined in Materials and Methods. Results for PZN and ASA are reported as mean of two independent measurements with criteria outlined in Materials and Methods. Grayed out cells marked with "dash" (-) indicate that depletion of the particular BA analyte was not observed or the depletion did not meet the criteria outlined in Materials and Methods.

DOI: 10.1021/acs.molpharmaceut.9b00562
Mol. Pharmaceutics 2019, 16, 4230−4240

d_4-TCDCA, which peaked at 3 h in the bile and the lysate, and d_4-GCA and d_4-TCA, which continued to increase in the supernatant until the end of the incubation. Amidation of secondary BAs peaked earlier between 1 and 24 h in all compartments; in contrast, HDCA was not amidated. Sulfation of primary BAs increased over time in all compartments throughout the duration of the experiment with the exception of d_4-CA-SO_4, which was not present in the bile nor the lysate. Sulfation of secondary BAs peaked between 1 and 3 h, but d_4-DCA-SO_4 and d_4-UDCA-SO_4 continued to increase over time in the supernatant. d_4-UDCA-SO_4 was also not found in the bile and the lysate. The profile of secondary metabolites (i.e., amidation and sulfation) varied depending on the BA species, and many of these secondary metabolites were not formed such as d_4-TCDCA-SO_4 and d_4-GUDCA-SO_4 in the bile and the lysate. On the basis of these differences in the concentration−time profile of BAs and their metabolites, it was reasoned that a single timepoint should not be used to compare between DMSO control and the perpetrating drugs TZN, PZN, and ASA. Instead, AUC was generated for each BA and its metabolites to compare between DMSO control and the perpetrating drugs.

Effect of TZN, PZN, and ASA on the Disposition of BAs and Their Metabolites in Vitro. The effect of TZN, PZN, or ASA on the disposition of BAs and their metabolites was investigated in lot HU1013. Figure S2A shows that the main metabolite for TZN was the sulfate conjugate and that TZN was completely depleted in the supernatant, bile, and lysate by 24 h. Figure S2B shows that the main metabolite for PZN was the hydroxylated metabolite. Unlike TZN, when PZN levels decreased over 72 h in the supernatant, it maintained relatively steady levels in the bile and the lysate. Figure S2C shows that ASA was immediately converted to salicylic acid, which underwent further metabolism to form salicyluric acid. Salicylic acid level was steady throughout the duration of the incubation in the supernatant, but peaked at 48 h in the bile and the lysate. When applicable, the degree of inhibition was captured by calculating IC_{50}s, and these values are summarized in Table 1 and the plots are shown in Figure S3. Criteria outlined in Materials and Methods were employed to ensure that IC_{50}s associated with good fits were reported.

In the presence of an ascending concentration of TZN, although the concentration of taurine conjugates did not change, the concentration of glycine conjugate d_4-GCA decreased in the bile with an IC_{50} of 16 ± 1 μM. In the lysate, d_4-GCA and d_4-GCDCA decreased with an IC_{50} of 5.6 ± 2.9 and 11 ± 12, respectively. Changes in the concentration of BA metabolites were accompanied by accumulation (i.e., >200% of DMSO control) of d_4-GLCA in the lysate and d_4-GDCA in the supernatant. In addition to glycine conjugates, sequential metabolites consisting of sulfate conjugates also decreased. In the lysate, IC_{50} of d_4-GCDCA-SO_4, d_4-GLCA-SO_4, and d_4-GDCA-SO_4 was 5.1 ± 2.1, 2.6 ± 0.7, and 3.9 ± 1.3 μM, respectively. In the supernatant, d_4-GCA−SO_4, d_4-GCDCA−SO_4, and d_4-GUDCA−SO_4 decreased with IC_{50} of 10 ± 6, 21 ± 12, and 26 ± 8 μM, respectively. No marked differences were observed in the bile. Similarly, in the presence of PZN, concentration of glycine conjugates d_4-GCA, d_4-GCDCA, and d_4-GUDCA decreased in the lysate with an IC_{50} value of 33 ± 32, 40 ± 12, and 19 ± 0.2 μM, respectively. This was accompanied by accumulation of d_4-GLCA in the lysate and d_4-GDCA in the supernatant. In addition, d_4-GCA−SO_4 and d_4-GCDCA−SO_4 in the supernatant decreased with IC_{50} of 27 ± 1 and 95 ± 49 μM, respectively, whereas d_4-GLCA−SO_4 and d_4-GDCA−SO_4 levels in the lysate decreased with IC_{50} of 35 ± 10 and 37 ± 26 μM, respectively. Unlike TZN, PZN was associated with reduction of d_4-UDCA in the lysate with IC_{50} of 74 ± 28 μM. In contrast to thiazolidinedione, ASA had no effect on the BA homeostasis. Figure 4 shows that TZN (up to 30 μM), PZN (up to 100 μM), and ASA (up to 1000 μM) were not associated with cytotoxicity or with poor viability.

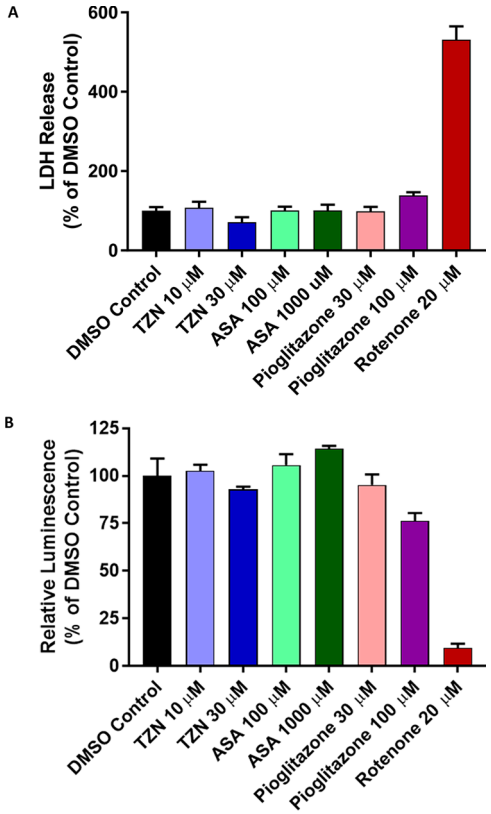

Figure 4. Viability and the cytotoxicity of TZN, PZN, and ASA determined with the (A) ATP luminescent and (B) LDH release assay in lot HU1013 (N = 3).

MPR of BAs that were modulated in the various compartments are shown in Figure 5. For BAs that were reduced and for which IC_{50}s were determined, the MPR was also reduced except for d_4-GCDCA−SO_4 with TZN and PZN in the lysate. For BAs that increased, the MPR also increased except for d_4-GLCA in the lysate for both TZN and PZN.

To investigate if the disruption of BA homeostasis was attributed to the particular lot (HU1013) and to assess the reproducibility of the findings, additional lots were examined. As observed with the previous lot HU1013, TZN interrupted BA homeostasis in lots HU1020 and HU1023. Table 2 (and plots shown in Figure S3) show that not only were similar BA species impacted by TZN, but that the IC_{50} values were comparable across the three different lots.

DISCUSSION

Assessing clinical disposition for hepatotoxicity is challenging because it can arise from the interplay between genetic, nongenetic, and/or environmental factors. It is further complicated because the assortment of preclinical tools has

DOI: 10.1021/acs.molpharmaceut.9b00562
Mol. Pharmaceutics 2019, 16, 4230−4240

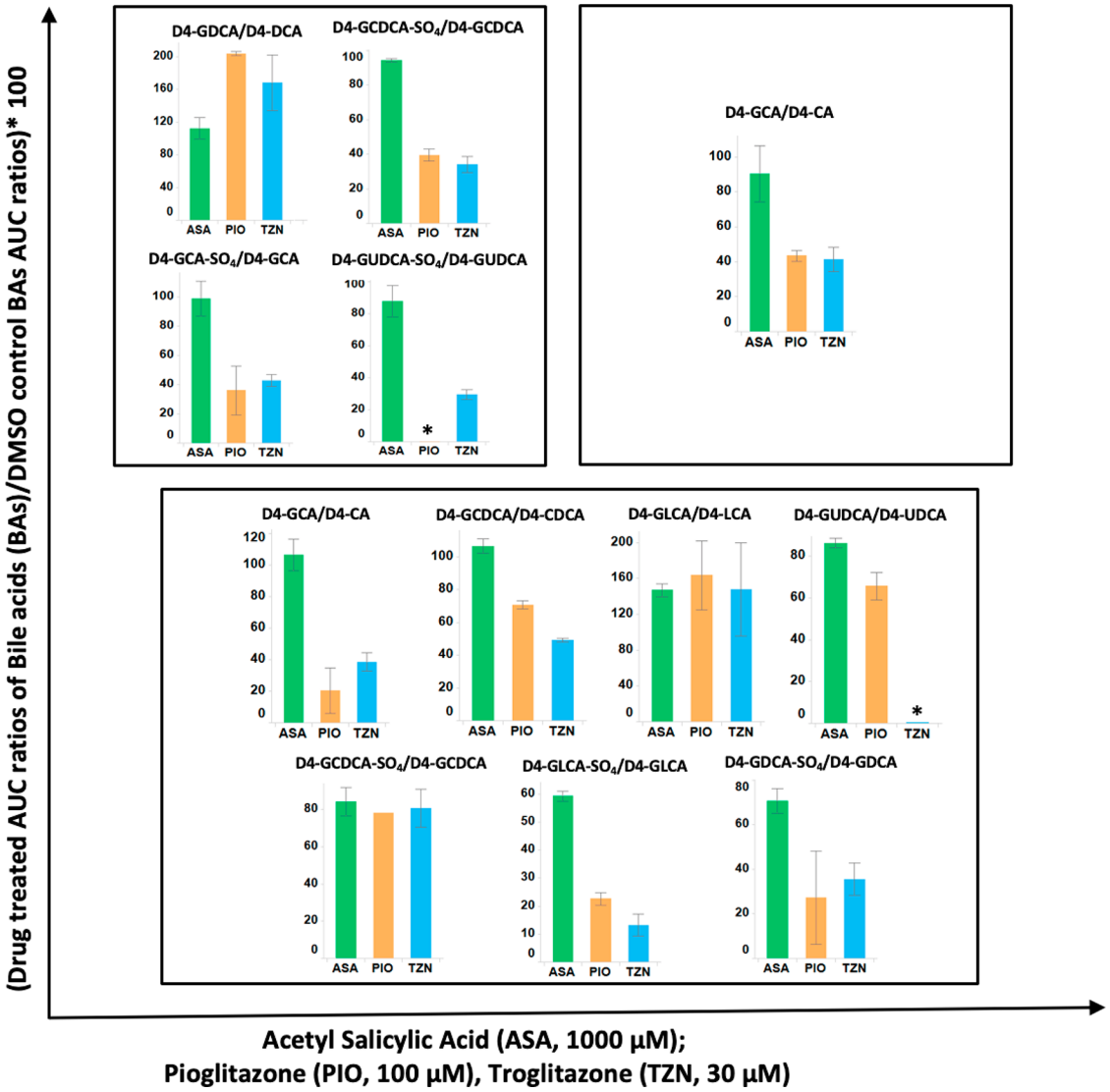

Figure 5. MPR were determined for BAs that were modulated in the supernatant (right box), bile (left box), and lysate (bottom box), in lot HU1013. MPR from the drug-treated group was normalized to their corresponding DMSO control and was calculated from AUC determined from 0 to 72 h. Black bars represent ASA (1000 μM, $N = 2$), gray bars represent PZN (100 μM, $N = 2$), and light gray bars represent TZN (30 μM, $N = 3$). The star symbol "*" represents the extent of inhibition being less than or equal to 50% of DMSO control.

yielded mediocre success in predicting clinical hepatotoxicity as the drivers which contribute to these factors remain elusive. One potential mechanism of hepatotoxicity is the interruption of BA homeostasis. Indeed, BAs have been linked to toxicity based on their hydrophobicity,[28] as well as their aptitude to cause apoptosis[29−31] or necrosis,[32,33] which may be dependent on whether BAs are enclosed by phospholipid micelles.[34] Therefore, modulation of BAs by drugs may be a prelude to the onset of DILI. The objective of this work was to investigate the effect of several compounds on the in vitro BA homeostasis in a long-enduring human hepatocyte co-culture system. TZN and PZN were chosen for this evaluation because DILI is well characterized with these molecules, and because they are both thiazolidinediones, they are associated with different clinical DILI profiles. ASA was the negative control as it is not commonly associated with DILI. The human hepatocyte co-culture was utilized because it offered several advantages to study BA disposition. In particular, Hurel exhibits both drug metabolizing enzyme and drug transporter activities over multiple days.[35−39] Hurel also forms functional bile canaliculi, which more closely mimics in vivo physiology and provides a dynamic environment where the hepatocytes can adapt to potential changes in BA homeostasis as needed, rather than only accumulating BAs intracellularly. Moreover, Hurel afforded an option to collect the supernatant, the lysate, and the bile within a single experiment, which enabled the examination of BA disposition in all compartments. Finally, based on our initial investigation with this system, it was found that at least 24 h of incubation was required in this system to completely capture BA metabolism such as sulfation.

Table 1 shows that in the presence of ASA, BA homeostasis was unaffected. In contrast, the concentration of certain glycine and sulfate conjugates in the presence of thiazolidinediones was markedly reduced. Meanwhile, large accumulation of d_4-GLCA and d_4-GDCA was observed in the lysate and supernatant, respectively, indicating that the in vitro system is maintaining mass balance, whereas the BA homeostasis is disrupted. Subsequent experiments in additional hepatocyte lots yielded comparable results, suggesting that interruption of BA homeostasis mediated by TZN was not a lot-specific effect

DOI: 10.1021/acs.molpharmaceut.9b00562
Mol. Pharmaceutics 2019, 16, 4230−4240

Table 2. Summary of Changes of the Concentration of Certain BAs and Their Metabolites Reported as IC_{50} (μM) in the Absence or Presence of Ascending Concentrations of TZN (0.1−30 μM) across Three Different Lots (HU1013, HU1023, and HU1020)[a]

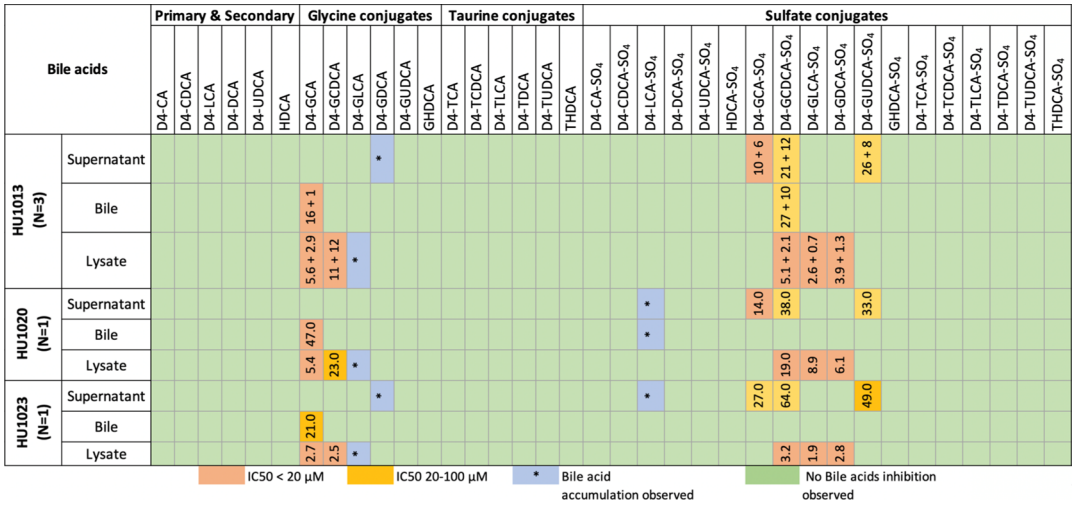

[a]Star (*) represents BAs or their metabolites which exhibited >200% accumulation over 72 h. Three independent measurements were taken with Lot HU1013 and the values are a mean ± SD of three independent measurements with criteria outlined in Materials and Methods. A single experiment was conducted with Lots HU1023 and HU1020, and the reported values fall within the criteria outlined in Materials and Methods. Grayed out cells marked with a "dash" (-) indicate that depletion of the particular BA analyte was not observed or the depletion did not meet the criteria outlined in Materials and Methods.

(Table 2). With the exception of d_4-GCDCA-SO_4, the corresponding changes in the MPR shown in Figure 5 indicate that the modulation of BAs was indeed because of changes in their metabolism. Moreover, Figure 4 shows that the hepatocytes were healthy, indicating that alterations of BAs were not due to poor condition of the hepatocytes. These data show that BA homeostasis was differentiated in the hepatocyte co-culture, where unlike ASA, thiazolidinediones were able to interrupt BA homeostasis by primarily reducing both glycine and sulfate conjugation. The effect on amidation and sulfation is important when considering detoxification of BAs. While enhancing solubility for more efficient elimination from the body, sulfation has been shown to diminish hepatotoxicity potential for LCA,[40] whereas less cytotoxicity has been attributed to glycine and taurine conjugates.[41] Therefore, although one mechanism of DILI for TZN has been hypothesized as inhibition against bile-salt export pump,[42] these data suggest that inhibition of glycine and sulfate conjugation may also contribute to DILI by reducing the extent of BA detoxification.

In vitro systems have been employed to study the potential relationship between BA and DILI. The results presented in this work add to the current knowledge by probing further into how thiazolidinediones may affect BA handling as it significantly expands on the panel of BAs in an in vitro system where the bile can be sampled along with the supernatant and the lysate. Previous works have evaluated a specific BA or a select set of BAs,[43,44] or assessed only the flux or metabolism of BAs,[45−47] or monitored a toxicity endpoint,[48,49] but this is the first work which details the handling of a comprehensive set of BAs in various spatial compartments. It has been demonstrated that glycination was the most prominent amidation biotransformation reaction,[48] and TZN significantly reduced amidation and sulfation of BAs.[50,51] Moreover, the majority of changes occurred in the lysate, and only few BAs were changed in the bile and the supernatant. The current work shows that TZN did not affect all glycine or sulfate conjugates, as the most effected sulfated species were GCDCA, GLCA, and GDCA, and glycinated species were CA and CDCA. In contrast, amidation of DCA and sulfation of LCA were not significantly altered. There are reports of successfully employing BA indices to profile certain liver diseases,[52,53] which may be appropriate as the entire architecture of the liver may change in a disease state. However, these findings suggest that changes in BAs will manifest in the serum and/or the urine for only a few specific BAs in the presence of thiazolidinediones to create a specific BA signature. Consequently, when considering BAs as biomarkers for DILI, rather than a nontarget approach, a targeted approach to assess imbalance in BA homeostasis is inferred. Moreover, this BA signature may vary depending on the mechanism of DILI, and a targeted analysis of BAs may help with data interpretation. More investigations are needed to evaluate the in vivo translatability of these data determined in the human hepatocyte co-cultures.

Although varying BA signatures were observed with different drugs in this system, it is worth recognizing that there are limitations to the current human hepatocyte co-culture system. For example, BA homeostasis is multifaceted and is also dependent on the gut microbiome metabolic activity and enterohepatic recirculation of BAs. Because the current work only investigates human hepatocytes in culture, the impact of drugs on the microbiome and enterohepatic recirculation of BAs are not captured. To partly circumvent this shortcoming, secondary BAs were supplemented to mirror physiologically relevant BA pool. Another drawback is that although the proportion of BA conjugation ranked ordered appropriately to what is reported in human serum, the extent of taurine conjugation was markedly lower than what is reported in human serum.[20] The likely reason is due to the low level of taurine as the expression of cysteine sulfinic acid decarboxylase, the rate-limiting step in the biosynthesis of taurine, is low.[54] In fact, much of taurine in humans comes from the diet.

DOI: 10.1021/acs.molpharmaceut.9b00562
Mol. Pharmaceutics 2019, 16, 4230−4240

Therefore, because taurine conjugation activity remained intact and because the extent of taurine conjugation in humans is also low, it was decided not to supplement it with exogenous taurine. One of the major limitations of the current system is that the human hepatocytes are co-cultured with mouse stromal cells. Preliminary data internally have indicated that mouse stromal cells exhibit glucuronidation activity; however, their contribution to BA disposition is unknown and further investigations are needed. Nevertheless, despite this caveat, there should be minimal impact to the current analysis such as with IC50 calculations with drugs as the BA profiles were compared with DMSO controls.

Because PZN and TZN are from the same drug class, it was not surprising that both were able to disrupt BA homeostasis. However, when compared to TZN, far fewer BAs were affected by PZN. Furthermore, for BAs that were impacted by both TZN and PZN, the IC_{50} values of TZN was 3- to 13-fold more potent. It has been implied that dose and exposure is important when considering in vitro inhibition data.[55,56] However, although the clinical C_{max} of TZN and PZN are similar at 6.3 μM[57] and 3.7 μM,[58] respectively, their doses that achieve these concentrations are different. Because C_{max} reflects postliver concentration, whereas the dose reflects preliver concentrations, C_{max} does not reflect how much drug the liver has processed. Instead, drug load may be more relevant when denoting drug burden to the liver and therefore, the more appropriate parameter to contextualize the in vitro IC_{50} values determined in the liver. Consequently, assuming stomach volume of 250 mL and complete absorption as assumed previously for both molecules,[59] the preliver concentration of 600 mg dose of TZN is approximately 5000 μM. In contrast, the preliver concentration of 45 mg dose of PZN is 10-fold lower at approximately 500 μM. Accordingly, this theoretical liver concentration of PZN is 10- to 25-fold of the IC_{50} values, whereas the theoretical liver concentration of TZN can be greater than 1000-fold of the IC_{50} values. The disparity in the coverage of the IC_{50} values by the theoretical liver concentration may explain the divergences in clinical instances of DILI, where TZN is more susceptible for DILI. These data suggest that PZN may also be prone to DILI, but only at higher doses.

In summary, an in vitro human hepatocyte system was characterized and optimized to evaluate BA homeostasis in the presence or absence of TZN, PZN, and ASA. This is one of the first studies using a dynamic in vitro system where a comprehensive panel of BAs was evaluated. In the presence of TZN and PZN, select glycine and sulfate conjugations were significantly modulated, whereas no effect was observed with ASA. The theoretical liver concentration of TZN was much higher against the IC_{50} values compared with the coverage afforded by PZN, which may explain differences in the clinical instances of DILI. This work shows that BA levels can be monitored in the human hepatocyte co-culture system, which may be used to elucidate potential mechanism of certain hepatotoxicities. It is worth noting that DILI-inducing drugs outside of the thiazolidinedione class have not yet been studied. For other drugs, it is possible that interruption of BA homeostasis may manifest in a different way, or may not change at all. Our laboratory is conducting experiments with other DILI-inducing drugs to collect their BA signatures in this system, which may provide insight into the mechanism and aid in identification of BAs to target in the clinic as a potential biomarker for liver injury.

■ ASSOCIATED CONTENT

Supporting Information

The Supporting Information is available free of charge on the ACS Publications website at DOI: 10.1021/acs.molpharmaceut.9b00562.

Representative concentration−time profile of all BAs and their conjugated metabolites; representative peak area−time profile of perpetrators TZN, PZN, and ASA their major metabolites; IC50 profiles of BAs in the presence of perpetrators TZN, PZN, and AZA (PDF)

■ AUTHOR INFORMATION

Corresponding Author

*E-mail: jaechang@gmail.com. Phone: (650) 467-9708. Fax: (650) 467-3487.

ORCID

Jae H. Chang: 0000-0003-3457-7695

Author Contributions

†These authors contributed equally to the paper.

Notes

The authors declare no competing financial interest.

■ ABBREVIATIONS

ASA, acetylsalicylic acid; AUC, area under the curve; BA, bile acid; CDCA, chenodeoxycholic acid; CA, cholic acid; DCA, deoxycholic acid; as prefix d_4-, deuterated; DILI, drug-induced liver injury; G, glycine; HRMS, high-resolution mass spectrometry; HDCA, hyodeoxycholic acid; LCA, lithocholic acid; PZN, pioglitazone; SO_4, sulfate; T, taurine; TZN, troglitazone; UHPLC, ultra-high-performance liquid chromatography; UDCA, ursodeoxycholic acid

■ REFERENCES

(1) Wilke, R. A.; Lin, D. W.; Roden, D. M.; Watkins, P. B.; Flockhart, D.; Zineh, I.; Giacomini, K. M.; Krauss, R. M. Identifying genetic risk factors for serious adverse drug reactions: current progress and challenges. *Nat. Rev. Drug Discovery* **2007**, *6*, 904−916.

(2) Lasser, K. E.; Allen, P. D.; Woolhandler, S. J.; Himmelstein, D. U.; Wolfe, S. M.; Bor, D. H. Timing of new black box warnings and withdrawals for prescription medications. *JAMA* **2002**, *287*, 2215−2220.

(3) Przybylak, K. R.; Cronin, M. T. In silico models for drug-induced liver injury–current status. *Expert Opin. Drug Metab. Toxicol.* **2012**, *8*, 201−217.

(4) Fraser, K.; Bruckner, D. M.; Dordick, J. S. Advancing Predictive Hepatotoxicity at the Intersection of Experimental, in Silico, and Artificial Intelligence Technologies. *Chem. Res. Toxicol.* **2018**, *31*, 412−430.

(5) Funk, C.; Roth, A. Current limitations and future opportunities for prediction of DILI from in vitro. *Arch. Toxicol.* **2017**, *91*, 131−142.

(6) Schadt, S.; Simon, S.; Kustermann, S.; Boess, F.; McGinnis, C.; Brink, A.; Lieven, R.; Fowler, S.; Youdim, K.; Ullah, M.; Marschmann, M.; Zihlmann, C.; Siegrist, Y. M.; Cascais, A. C.; Di Lenarda, E.; Durr, E.; Schaub, N.; Ang, X.; Starke, V.; Singer, T.; Alvarez-Sanchez, R.; Roth, A. B.; Schuler, F.; Funk, C. Minimizing DILI risk in drug discovery - A screening tool for drug candidates. *Toxicol. In Vitro* **2015**, *30*, 429−437.

(7) Howell, B. A.; Siler, S. Q.; Watkins, P. B. Use of a systems model of drug-induced liver injury (DILIsym) to elucidate the mechanistic differences between acetaminophen and its less-toxic isomer, AMAP, in mice. *Toxicol. Lett.* **2014**, *226*, 163−172.

(8) Olson, H.; Betton, G.; Robinson, D.; Thomas, K.; Monro, A.; Kolaja, G.; Lilly, P.; Sanders, J.; Sipes, G.; Bracken, W.; Dorato, M.; Van Deun, K.; Smith, P.; Berger, B.; Heller, A. Concordance of the

DOI: 10.1021/acs.molpharmaceut.9b00562
Mol. Pharmaceutics 2019, 16, 4230−4240

toxicity of pharmaceuticals in humans and in animals. *Regul. Toxicol. Pharmacol.* **2000**, *32*, 56−67.
(9) Rosenzweig, P.; Miget, N.; Brohier, S. Transaminase elevation on placebo during phase I trials: prevalence and significance. *Br. J. Clin. Pharmacol.* **1999**, *48*, 19−23.
(10) McKenzie, R.; Fried, M. W.; Sallie, R.; Conjeevaram, H.; Di Bisceglie, A. M.; Park, Y.; Savarese, B.; Kleiner, D.; Tsokos, M.; Luciano, C.; et al. Hepatic failure and lactic acidosis due to fialuridine (FIAU), an investigational nucleoside analogue for chronic hepatitis B. *N. Engl. J. Med.* **1995**, *333*, 1099−1105.
(11) Sjövall, J. Bile acids in man under normal and pathological conditions bile acids and steroids. *Clin. Chim. Acta* **1960**, *5*, 33−41.
(12) Vessey, D. A. The biochemical basis for the conjugation of bile acids with either glycine or taurine. *Biochem. J.* **1978**, *174*, 621−626.
(13) Barnes, S.; Gallo, G. A.; Trash, D. B.; Morris, J. S. Diagnositic value of serum bile acid estimations in liver disease. *J. Clin. Pathol.* **1975**, *28*, 506−509.
(14) Frosch, B.; Wagener, H. Quantitative determination of conjugated bile acids in serum in acute hepatitis. *Nature* **1967**, *213*, 404−405.
(15) Makino, I.; Nakagawa, S.; Mashimo, K. Conjugated and unconjugated serum bile acid levels n patients with hepatobiliary diseases. *Gastroenterology* **1969**, *56*, 1033−1039.
(16) Fausa, O.; Gjone, E. Serum bile acid concentrations in patients with liver disease. *Scand. J. Gastroenterol.* **1976**, *11*, 537−543.
(17) Bhushan, B.; Borude, P.; Edwards, G.; Walesky, C.; Cleveland, J.; Li, F.; Ma, X.; Apte, U. Role of bile acids in liver injury and regeneration following acetaminophen overdose. *Am. J. Pathol.* **2013**, *183*, 1518−1526.
(18) Fattinger, K.; Funk, C.; Pantze, M.; Weber, C.; Reichen, J.; Stieger, B.; Meier, P. J. The endothelin antagonist bosentan inhibits the canalicular bile salt export pump: a potential mechanism for hepatic adverse reactions. *Clin. Pharmacol. Ther.* **2001**, *69*, 223−231.
(19) Scherer, M.; Gnewuch, C.; Schmitz, G.; Liebisch, G. Rapid quantification of bile acids and their conjugates in serum by liquid chromatography-tandem mass spectrometry. *J. Chromatogr. B: Anal. Technol. Biomed. Life Sci.* **2009**, *877*, 3920−3925.
(20) Bathena, S. P. R.; Mukherjee, S.; Olivera, M.; Alnouti, Y. The profile of bile acids and their sulfate metabolites in human urine and serum. *J. Chromatogr. B: Anal. Technol. Biomed. Life Sci.* **2013**, *942*−*943*, 53−62.
(21) Sharanek, A.; Burban, A.; Humbert, L.; Bachour-El Azzi, P.; Felix-Gomes, N.; Rainteau, D.; Guillouzo, A. Cellular Accumulation and Toxic Effects of Bile Acids in Cyclosporine A-Treated HepaRG Hepatocytes. *Toxicol. Sci.* **2015**, *147*, 573−587.
(22) Boess, F.; Kamber, M.; Romer, S.; Gasser, R.; Muller, D.; Albertini, S.; Suter, L. Gene expression in two hepatic cell lines, cultured primary hepatocytes, and liver slices compared to the in vivo liver gene expression in rats: possible implications for toxicogenomics use of in vitro systems. *Toxicol. Sci.* **2003**, *73*, 386−402.
(23) Tchaparian, E. H.; Houghton, J. S.; Uyeda, C.; Grillo, M. P.; Jin, L. X. Effect of Culture Time on the Basal Expression Levels of Drug Transporters in Sandwich-Cultured Primary Rat Hepatocytes. *Drug Metab. Dispos.* **2011**, *39*, 2387−2394.
(24) Hurel. *Hurelflux Biliary Efflux Assay Method Sample Protocol: Taurocholate (TA)*; Hurel Corporation.
(25) Bachmann, A.; Moll, M.; Gottwald, E.; Nies, C.; Zantl, R.; Wagner, H.; Burkhardt, B.; Sanchez, J. J.; Ladurner, R.; Thasler, W.; Damm, G.; Nussler, A. K. 3D Cultivation Techniques for Primary Human Hepatocytes. *Microarrays* **2015**, *4*, 64−83.
(26) Bell, C. C.; Dankers, A. C. A.; Lauschke, V. M.; Sison-Young, R.; Jenkins, R.; Rowe, C.; Goldring, C. E.; Park, K.; Regan, S. L.; Walker, T.; Schofield, C.; Baze, A.; Foster, A. J.; Williams, D. P.; van de Ven, A. W. M.; Jacobs, F.; Houdt, J. V.; Lahteenmaki, T.; Snoeys, J.; Juhila, S.; Richert, L.; Ingelman-Sundberg, M. Comparison of Hepatic 2D Sandwich Cultures and 3D Spheroids for Long-term Toxicity Applications: A Multicenter Study. *Toxicol. Sci.* **2018**, *162*, 655−666.
(27) Godoy, P.; Hewitt, N. J.; Albrecht, U.; Andersen, M. E.; Ansari, N.; Bhattacharya, S.; Bode, J. G.; Bolleyn, J.; Borner, C.; Böttger, J.; Braeuning, A.; Budinsky, R. A.; Burkhardt, B.; Cameron, N. R.; Camussi, G.; Cho, C. S.; Choi, Y. J.; Craig Rowlands, J.; Dahmen, U.; Damm, G.; Dirsch, O.; Donato, M. T.; Dong, J.; Dooley, S.; Drasdo, D.; Eakins, R.; Ferreira, K. S.; Fonsato, V.; Fraczek, J.; Gebhardt, R.; Gibson, A.; Glanemann, M.; Goldring, C. E.; Gómez-Lechón, M. J.; Groothuis, G. M.; Gustavsson, L.; Guyot, C.; Hallifax, D.; Hammad, S.; Hayward, A.; Häussinger, D.; Hellerbrand, C.; Hewitt, P.; Hoehme, S.; Holzhütter, H. G.; Houston, J. B.; Hrach, J.; Ito, K.; Jaeschke, H.; Keitel, V.; Kelm, J. M.; Kevin Park, B.; Kordes, C.; Kullak-Ublick, G. A.; LeCluyse, E. L.; Lu, P.; Luebke-Wheeler, J.; Lutz, A.; Maltman, D. J.; Matz-Soja, M.; McMullen, P.; Merfort, I.; Messner, S.; Meyer, C.; Mwinyi, J.; Naisbitt, D. J.; Nussler, A. K.; Olinga, P.; Pampaloni, F.; Pi, J.; Pluta, L.; Przyborski, S. A.; Ramachandran, A.; Rogiers, V.; Rowe, C.; Schelcher, C.; Schmich, K.; Schwarz, M.; Singh, B.; Stelzer, E. H.; Stieger, B.; Stober, R.; Sugiyama, Y.; Tetta, C.; Thasler, W. E.; Vanhaecke, T.; Vinken, M.; Weiss, T. S.; Widera, A.; Woods, C. G.; Xu, J. J.; Yarborough, K. M.; Hengstler, J. G. Recent advances in 2D and 3D in vitro systems using primary hepatocytes, alternative hepatocyte sources and non-parenchymal liver cells and their use in investigating mechanisms of hepatotoxicity, cell signaling and ADME. *Arch. Toxicol.* **2013**, *87*, 1315−1530.
(28) Attili, A. F.; Angelico, M.; Cantafora, A.; Alvaro, D.; Capocaccia, L. Bile acid-induced liver toxicity: relation to the hydrophobic-hydrophilic balance of bile acids. *Med. Hypotheses* **1986**, *19*, 57−69.
(29) Patel, T.; Bronk, S. F.; Gores, G. J. Increases of intracellular magnesium promote glycodeoxycholate-induced apoptosis in rat hepatocytes. *J. Clin. Invest.* **1994**, *94*, 2183−2192.
(30) Rodrigues, C. M.; Fan, G.; Ma, X.; Kren, B. T.; Steer, C. J. A novel role for ursodeoxycholic acid in inhibiting apoptosis by modulating mitochondrial membrane perturbation. *J. Clin. Invest.* **1998**, *101*, 2790−2799.
(31) Yerushalmi, B.; Dahl, R.; Devereaux, M. W.; Gumpricht, E.; Sokol, R. J. Bile acid-induced rat hepatocyte apoptosis is inhibited by antioxidants and blockers of the mitochondrial permeability transition. *Hepatology* **2001**, *33*, 616−626.
(32) Galle, P. R.; Theilmann, L.; Raedsch, R.; Otto, G.; Stiehl, A. Ursodeoxycholate reduces hepatotoxicity of bile salts in primary human hepatocytes. *Hepatology* **1990**, *12*, 486−491.
(33) Sokol, R. J.; Winklhofer-Roob, B. M.; Devereaux, M. W.; McKim, J. M., Jr. Generation of hydroperoxides in isolated rat hepatocytes and hepatic mitochondria exposed to hydrophobic bile acids. *Gastroenterology* **1995**, *109*, 1249−1256.
(34) Smit, J. J.; Schinkel, A. H.; Oude Elferink, R. P.; Groen, A. K.; Wagenaar, E.; van Deemter, L.; Mol, C. A.; Ottenhoff, R.; van der Lugt, N. M.; van Roon, M. A.; et al. Homozygous disruption of the murine mdr2 P-glycoprotein gene leads to a complete absence of phospholipid from bile and to liver disease. *Cell* **1993**, *75*, 451−462.
(35) Novik, E.; Maguire, T. J.; Chao, P.; Cheng, K. C.; Yarmush, M. L. A microfluidic hepatic coculture platform for cell-based drug metabolism studies. *Biochem. Pharmacol.* **2010**, *79*, 1036−1044.
(36) Novik, E.; Shipton, M.; Parekh, A.; Cho, C.; Pludwinski, E.; Shrirao, A. *Characterizing Hepato-Biliary Transport Utilizing the Stable, Long-Enduring Cellular Competency of Hurel(R) Co-Culture Technology and Single-Well Direct Assay Method, 13th European ISSX Meeting*, Glasgow, Scotland, 2015.
(37) HμRELflux Biliary Efflux Assay Kit; Frequently Asked Questions (FAQ's).
(38) Kidambi, S.; Yarmush, R. S.; Novik, E.; Chao, P.; Yarmush, M. L.; Nahmias, Y. Oxygen-mediated enhancement of primary hepatocyte metabolism, functional polarization, gene expression, and drug clearance. *Proc. Natl. Acad. Sci. U.S.A.* **2009**, *106*, 15714−15719.
(39) Kratochwil, N. A.; Meille, C.; Fowler, S.; Klammers, F.; Ekiciler, A.; Molitor, B.; Simon, S.; Walter, I.; McGinnis, C.; Walther, J.; Leonard, B.; Triyatni, M.; Javanbakht, H.; Funk, C.; Schuler, F.; Lave, T.; Parrott, N. J. Metabolic Profiling of Human Long-Term Liver

DOI: 10.1021/acs.molpharmaceut.9b00562
Mol. Pharmaceutics 2019, 16, 4230−4240

Models and Hepatic Clearance Predictions from In Vitro Data Using Nonlinear Mixed-Effects Modeling. *AAPS J.* **2017**, *19*, 534−550.
(40) Palmer, R. H.; Bolt, M. G. Bile acid sulfates. I. Synthesis of lithocholic acid sulfates and their identification in human bile. *J. Lipid Res.* **1971**, *12*, 671−679.
(41) Sharma, R.; Majer, F.; Peta, V. K.; Wang, J.; Keaveney, R.; Kelleher, D.; Long, A.; Gilmer, J. F. Bile acid toxicity structure-activity relationships: correlations between cell viability and lipophilicity in a panel of new and known bile acids using an oesophageal cell line (HET-1A). *Bioorg. Med. Chem.* **2010**, *18*, 6886−6895.
(42) Funk, C.; Ponelle, C.; Scheuermann, G.; Pantze, M. Cholestatic potential of troglitazone as a possible factor contributing to troglitazone-induced hepatotoxicity: in vivo and in vitro interaction at the canalicular bile salt export pump (Bsep) in the rat. *Mol. Pharmacol.* **2001**, *59*, 627−635.
(43) Marion, T. L.; Perry, C. H.; St Claire, R. L., 3rd; Brouwer, K. L. Endogenous bile acid disposition in rat and human sandwich-cultured hepatocytes. *Toxicol. Appl. Pharmacol.* **2012**, *261*, 1−9.
(44) Liu, J.; Lu, H.; Lu, Y.-F.; Lei, X.; Cui, J. Y.; Ellis, E.; Strom, S. C.; Klaassen, C. D. Potency of individual bile acids to regulate bile acid synthesis and transport genes in primary human hepatocyte cultures. *Toxicol. Sci.* **2014**, *141*, 538−546.
(45) Zhang, J.; He, K.; Cai, L.; Chen, Y.-C.; Yang, Y.; Shi, Q.; Woolf, T. F.; Ge, W.; Guo, L.; Borlak, J.; Tong, W. Inhibition of bile salt transport by drugs associated with liver injury in primary hepatocytes from human, monkey, dog, rat, and mouse. *Chem.-Biol. Interact.* **2016**, *255*, 45−54.
(46) Qiu, X.; Zhang, Y.; Liu, T.; Shen, H.; Xiao, Y.; Bourner, M. J.; Pratt, J. R.; Thompson, D. C.; Marathe, P.; Humphreys, W. G.; Lai, Y. Disruption of BSEP Function in HepaRG Cells Alters Bile Acid Disposition and Is a Susceptive Factor to Drug-Induced Cholestatic Injury. *Mol. Pharmaceutics* **2016**, *13*, 1206−1216.
(47) Ansede, J. H.; Smith, W. R.; Perry, C. H.; St Claire, R. L., 3rd; Brouwer, K. R. An in vitro assay to assess transporter-based cholestatic hepatotoxicity using sandwich-cultured rat hepatocytes. *Drug Metab. Dispos.* **2010**, *38*, 276−280.
(48) Chatterjee, S.; Richert, L.; Augustijns, P.; Annaert, P. Hepatocyte-based in vitro model for assessment of drug-induced cholestasis. *Toxicol. Appl. Pharmacol.* **2014**, *274*, 124−136.
(49) Oorts, M.; Richert, L.; Annaert, P. Drug-induced cholestasis detection in cryopreserved rat hepatocytes in sandwich culture. *J. Pharmacol. Toxicol. Methods* **2015**, *73*, 63−71.
(50) Ogimura, E.; Nakagawa, T.; Deguchi, J.; Sekine, S.; Ito, K.; Bando, K. Troglitazone Inhibits Bile Acid Amidation: A Possible Risk Factor for Liver Injury. *Toxicol. Sci.* **2017**, *158*, 347−355.
(51) Sharanek, A.; Burban, A.; Humbert, L.; Guguen-Guillouzo, C.; Rainteau, D.; Guillouzo, A. Progressive and Preferential Cellular Accumulation of Hydrophobic Bile Acids Induced by Cholestatic Drugs Is Associated with Inhibition of Their Amidation and Sulfation. *Drug Metab. Dispos.* **2017**, *45*, 1292−1303.
(52) Bathena, S. P. R.; Thakare, R.; Gautam, N.; Mukherjee, S.; Olivera, M.; Meza, J.; Alnouti, Y. Urinary bile acids as biomarkers for liver diseases II. Signature profiles in patients. *Toxicol. Sci.* **2015**, *143*, 308−318.
(53) Huang, W. M.; Seubert, D. E.; Donnelly, J. G.; Liu, M.; Javitt, N. B. Intrahepatic cholestasis of pregnancy: detection with urinary bile acid assays. *J. Perinat. Med.* **2007**, *35*, 486−491.
(54) Reymond, I.; Sergeant, A.; Tappaz, M. Molecular cloning and sequence analysis of the cDNA encoding rat liver cysteine sulfinate decarboxylase (CSD). *Biochim. Biophys. Acta* **1996**, *1307*, 152−156.
(55) Chang, J. H.; Plise, E.; Cheong, J.; Ho, Q.; Lin, M. Evaluating the in vitro inhibition of UGT1A1, OATP1B1, OATP1B3, MRP2, and BSEP in predicting drug-induced hyperbilirubinemia. *Mol. Pharmaceutics* **2013**, *10*, 3067−3075.
(56) Obach, R. S.; Kalgutkar, A. S.; Soglia, J. R.; Zhao, S. X. Can in vitro metabolism-dependent covalent binding data in liver microsomes distinguish hepatotoxic from nonhepatotoxic drugs? An analysis of 18 drugs with consideration of intrinsic clearance and daily dose. *Chem. Res. Toxicol.* **2008**, *21*, 1814−1822.
(57) Spencer, C. M.; Markham, A. Troglitazone. *Drugs* **1997**, *54*, 89−101 ; discussion 102 .
(58) Budde, K.; Neumayer, H.-H.; Fritsche, L.; Sulowicz, W.; Stompôr, T.; Eckland, D. The pharmacokinetics of pioglitazone in patients with impaired renal function. *Br. J. Clin. Pharmacol.* **2003**, *55*, 368−374.
(59) Izumi, T.; Enomoto, S.; Hosiyama, K.; Sasahara, K.; Shibukawa, A.; Nakagawa, T.; Sugiyama, Y. Prediction of the human pharmacokinetics of troglitazone, a new and extensively metabolized antidiabetic agent, after oral administration, with an animal scale-up approach. *J. Pharmacol. Exp. Ther.* **1996**, *277*, 1630−1641.

DOI: 10.1021/acs.molpharmaceut.9b00562
Mol. Pharmaceutics 2019, 16, 4230−4240